Stray Current Affects the Release of Bound Chloride Ions in Hydrated Cement Paste

Chonggen Pan[1], Jian Geng[1], Qingjun Ding[2]*

[1] Research Center of Green Building Materials and Waste Resources Reuse, Ningbo Institute of Technology, Zhejiang University, China
[2] School of Materials Science and Engineering, Wuhan University of Technology, China
*E-mail: gengjian@whut.edu.cn

Here, the effect of stray current on the release of bound chloride ions was evaluated using applied direct current (DC). Stray current induced the release of bound chloride ions, which escalated with both increasing loading time and voltage. The release of bound chloride ions in hydrated cement paste (HCP) was attributed to the release of chloride ions that had been adsorbed by the C-S-H gel. Owing to their attraction in the stray current's electrical field, adsorbed chloride ions in the electrical double layer(EDL) of the C-S-H gel—including both Stern and diffusion layers—were released. This also resulted in an increased zeta potential (ζ) of the C-S-H gel surface. Since the EDL thickness will gradually thin due to the stray current's electrical field, the amount of chloride ions re-entering the EDL will decrease after the stray current is stopped. Given this, there is a long-term, negative effect of stray current on the stability of bound chloride ions in hydrated cement paste.

Keywords: Stray current; Bound chlorides; C-S-H gel; Electrical double layer; Zeta potential

1. INTRODUCTION

Concrete contains both free and bound forms of chlorine, with the latter being bound through either chemical reactions and/or physical adsorption. Chemical reactions allow for calcium chloride to form, which is predominantly bound in Friedel's salt (FS) ($3CaO \cdot Al_2O_3 \cdot CaCl_2 \cdot 10H_2O$). During physical adsorption, chloride ions are primarily adsorbed by calcium silicate hydrate (C-S-H). However, recent work has shown that bound chloride is not static and can be released due to attack by sulfate solutions and/or carbonation [1-5]. As a result, free chloride in the poured concrete solution can increase, leading to more serious corrosion of reinforced concrete. Given this, it is critically important to understand the induction and mechanism behind chloride ion release.

During the past decade, the development of urban railway transportation systems across China has been incredibly rapid. As a result, there are now more than thirty cities that have urban railway transportation systems—most of which are based on reinforced concrete. When compared with other infra structure systems, these structures have additional durability problems. In particular, the fact that stray current can induce corrosion through reinforced concrete. Owing to the impedance difference between train track and concrete, stray current is common in the concrete structure of urban railway networks [6]. Depending on the source, stray current represents current leakage and may be from either direct (DC) or alternating (AC) currents. While both can result in metal corrosion, past work has shown that stray DC can result in more serious corrosion when compared with AC [7-12].

When current flows through reinforced concrete, electrical fields are formed. These fields likely affect the ions in the pore solution of the concrete. This can not only affect ion migration [13-15], but also the chloride binding capacity within the concrete itself [16]. Within cement chemistry, it is widely thought that C-S-H gel adsorption of chloride ions is related to the EDL [17-20]. Given this, it is reasonable to hypothesize that stray current can affect the stability of bound chloride ions in a C-S-H gel. Despite robust work examining the changing character of chloride ion release in concrete under different environmental conditions [1-5], little work has been done regarding the effect of stray current on the release of bound chloride ions.

Most parts of the concrete structures used in urban railway networks are at great depths from the surface. As a result, stray DC current and chloride ions in the ground water frequently coexist. Here, we focus on the effect of stray current on the release of bound chloride ions. Bound chloride ion stability in cement pastes, FS, and C-S-H gels were examined by analyzing the change in bound chloride ions of samples after they were exposed to DC. The mechanisms behind bound chloride ion release in tested samples were also analyzed and are discussed based on changes to their respective Zeta potentials (ζ).

2. MATERIALS AND METHODS

2.1 Materials

The cement used in this research was Type 42.5 Ordinary Portland Cement (OPC) made in Yadong Cement Company, Hubei, China. The chemical composition of OPC is listed in Table 1. In all experiments presented here, 0.5 MNaCl consisting of distilled water and reagent-grade NaCl were used in conjunction with the OPC. The mass ratio of water to cement was 0.3.

Table 1. Chemical composition of main materials   (data presented by mass %)

	SiO_2	CaO	MgO	Fe_2O_3	Al_2O_3	SO_3	Ignition loss
OPC	20.47	59.64	3.74	4.80	5.90	2.08	2.44

2.2 Methods

All cement pastes were cylindrical in shape with a diameter of ϕ 50×160 mm. Round steel with a diameter of ϕ 9×160 mm was embedded in every sample, the top of which was 2 cm from the

sample's surface. All samples were cured at standard curing conditions (20±2°C and 95% relative humidity for 28 d. Samples were then subjected to DC for to assess the effects of stray current. The experimental apparatus is shown in Fig. 1. Briefly, aplastic container served as the tank and was filled with an electrolytic solution (3% w/v NaOH). The polar plate was made of stainless steel and was placed below the sample. DC was introduced from the right side of the tank, where the anode was connected to the round steel of the sample and the cathode to the polar plate. Past work by Chen and colleagues monitored stray current intensity within gas pipelines of the Shanghai underground, which revealed that current intensity was approximately 100 mA [11]. Given this and in order to simulate an appropriate amount of stray current, different DC voltages (30, 20, 10, and 5 V) were applied to control current intensity. The resulting change in current intensity ranged from 20 to 100 mA.

Two methods were used for DC application. The first approach used a constant application of 20 V DC for 1, 2, 4, 6, and 14 d to investigate the effect of current application time on the stability of bound chloride ions. The second approach used a constant application of 20 V DC for 4 d. Samples were then re-cured at standard curing conditions for 7, 14, 28, and 56 consecutive days to investigate changes to the quantity of bound chloride ions after cessation of DC. Only samples in the second approach were subjected to all four timeframes of re-curing. It should be noted that expanded cracks on a given sample's surface formed due to corrosion of the embedded round steel. This can lead to rapid permeation of the electrolytic NaOH solution. Given this, all samples' surfaces—with the exception for the top and bottom—were covered by PVC modeling until the experiment was completed. After the conclusion of the experiment, all samples were broken into small sections and immersed in anhydrous ethanol for 7 days to terminate hydration. It is also worth noting that the generation of an electrical field induces free chloride ions to gather near the surface of the round steel. Given this, sections that were next to the round steel were excluded for chloride ion content titration. Sections that were contaminated by rust were also excluded. Finally, selected sections were then ground into a fine powder and passed through a sieve of 0.15 mm mesh aperture size for later chloride ion content titration and micro-analyses.
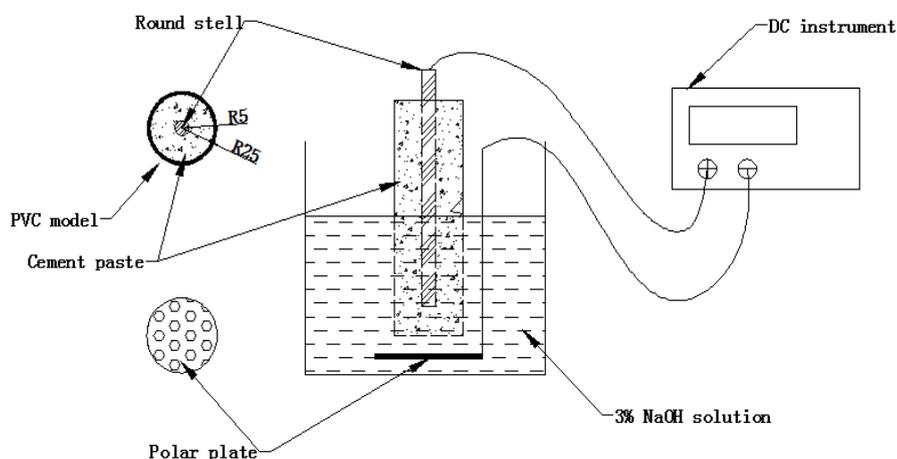
Figure 1. The sketch of the apparatus for stray current experiment

Pure tricalcium aluminate ($3CaO \cdot Al_2O_3$ (C_3A)) was made using a 1:3 molar ratio of reagent grade Al_2O_3 to CaO. This mixture was then repeatedly heated to 1400°C until the quantity of free CaO in C_3A was lower than 1%. The C_3A X-ray diffraction (XRD) pattern is shown in Fig.2. After heating, a mixture of now-pure C_3A powder and 0.5 M NaCl solution was made (0.3 w/v ratio of solid to solution). This mixture was then cast into a $^\phi$ 30×100 mm diameter PVC model and the stainless-steel rod was embedded (Fig.1). After 14 d of curing at standard curing conditions, samples were subjected to DC to investigate the effect of stray current on the stability of Friedel's salt(FS). These FSstray current experiments were divided into two sets. The first set of samples were subjected to 10 V DC for 1, 4, and 6 d, while the second were loaded with DC for 4 d at different voltages (5, 10, or 15 V). The resulting 14 d hydration product XRD patterns for C_3A and 0.5 M NaCl are shown in Fig.3.
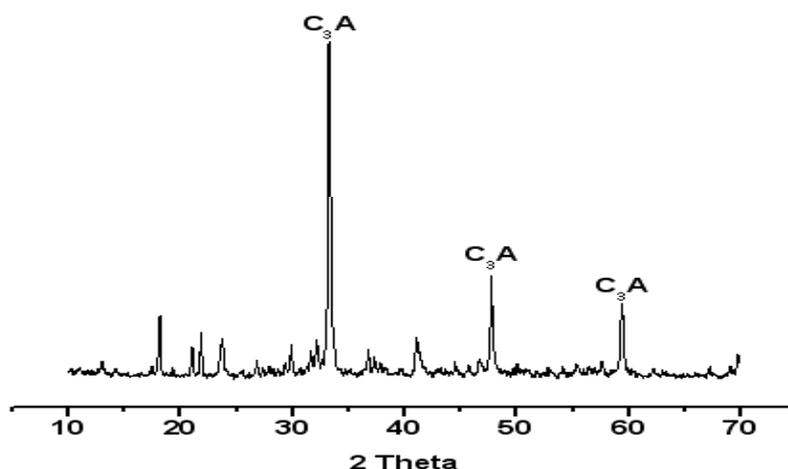
Figure 2. The XRD pattern of pure C_3A made with a 1:3 molar ratio mixture of reagent grades of Al_2O_3 and CaO, and repeatedly heated at 1400°C
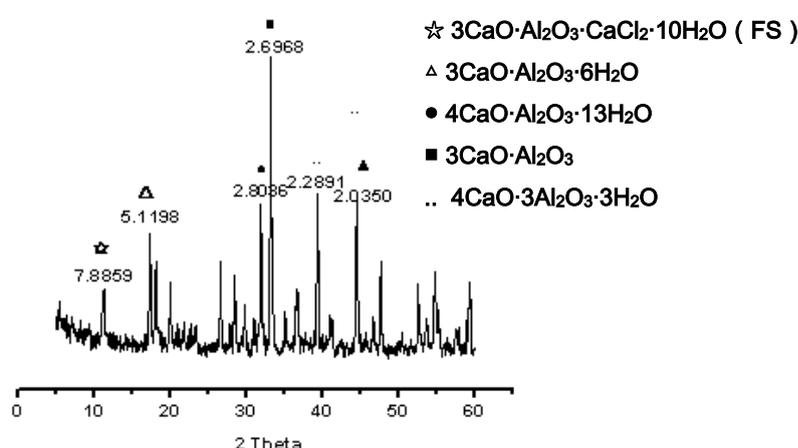
Figure 3. The XRD pattern of the hydration products of C_3A and 0.5 mol/L NaCl solution for 14 day

Pure C-S-H gel was synthesized using chemical precipitation. First, two separate, saturated solutions were made using reagent-grade $Ca(NO)_3 \cdot 4H_2O$ and $NaSiO_3 \cdot 9H_2O$, respectively. Next, these two solutions were mixed at a 1.8 molar ratio of Ca to Si. The resulting solution was then cured at

room temperature (20±2℃) for 15 d. The subsequent precipitate formed in the solution was repeatedly washed using deionized water to remove free ions in the C-S-H gel. The precipitate was then immersed in 0.5 M NaOH for 14 d, after which, the C-S-H gel was dried in a drying vessel for 7 d. The resulting C-S-H gel had a 1:50 mass ratio of solid to solution and was immersed in 0.5 M NaCl for 1, 7, and 14 d. Only C-S-H gels that had been immersed in NaCl solution for 7 d were used in all subsequent stray current experiments. The stray current experimental methodology for C-S-H gels was the same as that for FS. The SEM images and XRD patterns of C-S-H formed using chemical precipitation are show in Figs. 4 and 5, respectively.
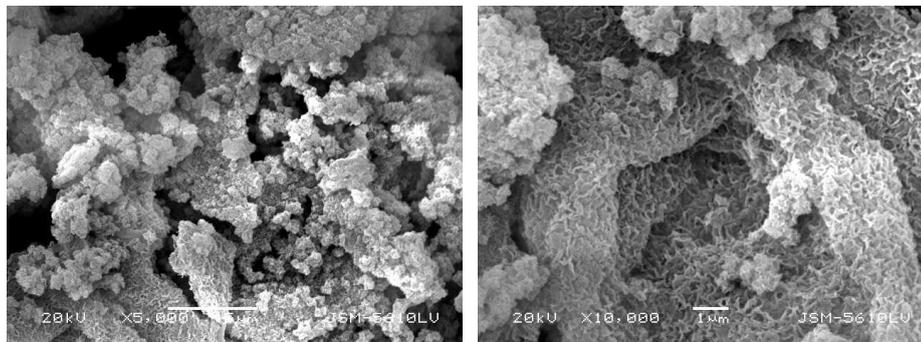
Figure 4. The SEM image of C-S-H gel synthesized by the way of chemical precipitation
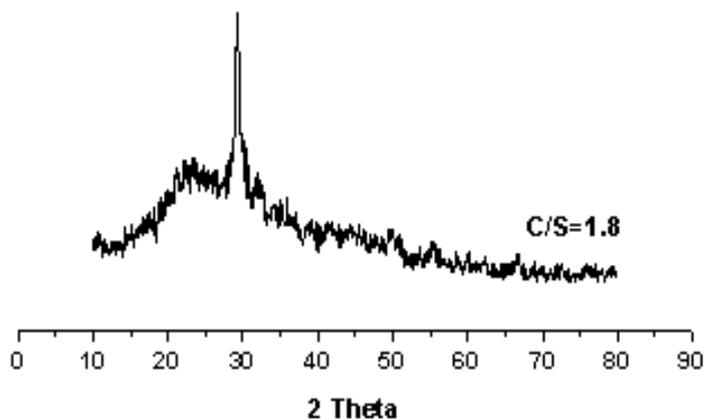
Figure 5. The XRD pattern of C-S-H synthesized by the way of chemical precipitation

The total chloride content (C_t) of the sample cured at standard curing condition was calculated based on the amount of mixing water made using the 0.5 M NaCl solution (5.318 mg/g). The free chloride content (C_f) was measured using the traditional leaching method in accordance with the standard presented by the Test Code for Hydraulic Concrete (SL352-2006). A dimensionless index, R_{cl}, was used to analyze the stability of bound chloride ions. It represented the mass ratio of bound chloride ions to the total initial chloride ions and was defined as follows:

$$R_{cl} = \frac{(C_t - C_f)}{5.318}\%$$

(1)

Where 5.318 mg/g was the total chloride ion content in the sample.

XRD was carried out using a RigakuD/Max-RB instrument that generated Cu Kα radiation of 40 kV and 30 mA. The diffraction spectra were collected within a scale range of 5-60^o(2θ) and with a step size of 0.02^o/s.

A suspension liquid with a 1:100 mass ratio of the dry sample to distilled water was used for all ζ measurements. Before all measurements, the suspension was maintained at room temperature for 1h. It was then dispersed using ultrasonic waves for 1 min. ζ was then measured using a BDL-B zeta sizer nano. ζ results are given as the mean value of five separate measurements per sample.

3. RESULTS

3.1 Stability of bound chloride ions in hydrated cement paste (HCP)

The effect of stray current loading time and voltage on the stability of bound chloride ions in HCP, FS, and C-S-H is shown in Figs.6 and 7. As shown in Fig. 6, the application of 20 V DC to HCP resulted in a marked decrease of R_{cl} values overloading time from 0 to 4 d. After day 4, the decrease in R_{cl} slowed from 12.39% at 4 d to 11.08% at 14 d. As shown in Fig.7, HCP R_{cl} values decreased with increasing voltage. However, it was apparent that the effect of stray current on the change in R_{cl} values was not notable when DC voltage was only 5 V. In this study, total chloride ion content in all samples was constant. Given this, the observed decrease in HCP R_{cl} values (Figs.6 and 7) indicated that stray current resulted in the release of bound chloride ions.

Fig. 7 shows the change in HCP R$_{cl}$ values, which were re-cured at standard curing conditions for 7, 14, 28, and 56 consecutive days after the application of 20 V DC for 4 d. As expected, there was an increase in R_{cl} values over consecutive days. This suggested that released chloride ions were re-bound after the stray current was removed. However, the highest HCP R_{cl} value after it was re-cured for 56 d (Fig. 8) was still lower than that observed before DC application. Given this, it can be concluded that there was a long-term effect of stray current on the stability of bound chloride ions.
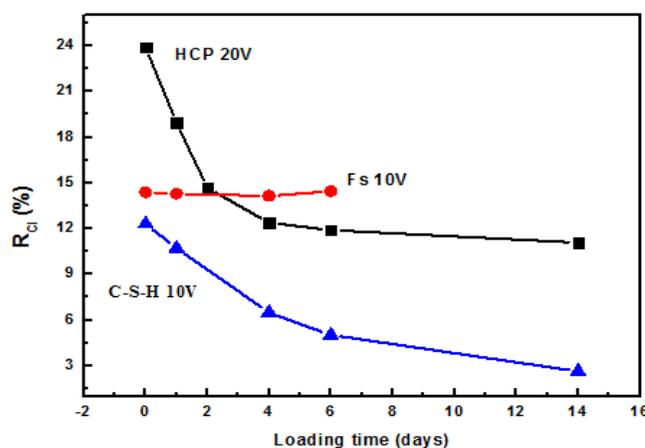
Figure 6. The effect of loading time of stray current on the stability of bound chlorides
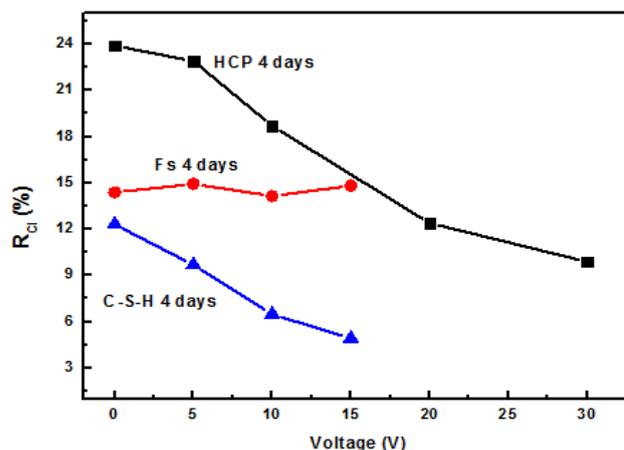
Figure 7. The effect of voltage of stray current on the stability of bound chlorides
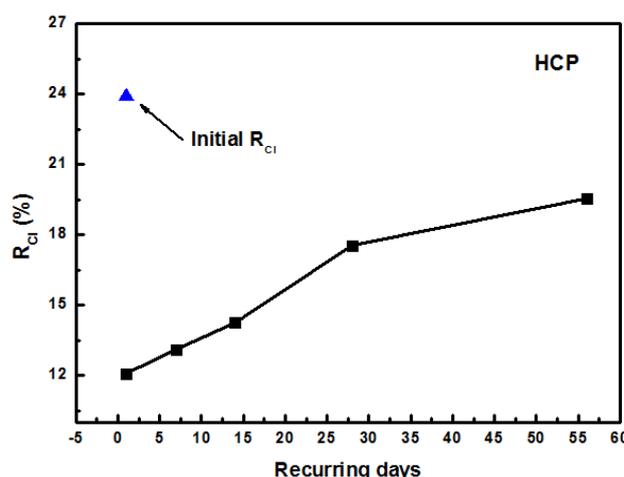
Figure 8. The relationship between the recurring days and R_{Cl}

3.2 Release of chloride ions in FS

As shown in Fig.6, when DC application time increased from 0 to 6 d, FS R_{cl} values varied from 14.39% to 14.45%. This variation was essentially negligible when compared with those values obtained for HCP. Moreover, increasing DC voltage had no obvious effects on FS R_{cl} values, which varied from 14.39% at 0 V to 14.82% at 15V (Fig. 8). This finding suggests that FS stability is independent of stray current.

Here, NaCl solution was used as the mixing water. With this in mind, FS derived not only from the chemical reaction between NaCl and C_3A, but also between NaCl and mono-sulfoaluminate (AFm)—the C_3A hydration product. As such, the FS formation process can be given by Eqs.(2)-(4) [21][22]:

$$Ca(OH)_2 + 2NaCl \rightarrow CaCl_2 + 2Na^+ + 2OH^- \tag{2}$$

$$3CaO \cdot Al_2O_3 + CaCl_2 + 10H_2O \rightarrow 3CaO \cdot Al_2O_3 \cdot CaCl_2 \cdot 10H_2O (FS) \tag{3}$$

$$3CaO \cdot Al_2O_3 \cdot CaSO_4 \cdot 12H_2O(AFm) + 2NaCl$$
$$\rightarrow 3CaO \cdot Al_2O_3 \cdot CaCl_2 \cdot 10H_2O(FS) + 2Na^+ + SO_4{}^{2-} + 2H_2O \qquad (4)$$
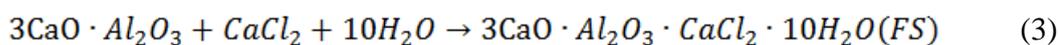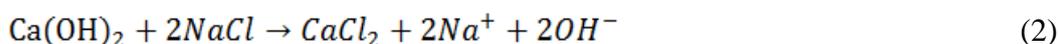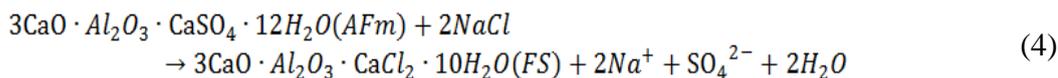
FS structure features electrostatic attraction between Cl^- and Ca^{2+} ions, ultimately resulting in ionic bonding. As a result, Cl^- can continuously exist in the structure of FS. It is now known that the stability of bound chloride ions when found in FS is dependent on both the alkalinity of the pore solution as well as temperature. FS dissolution can thus be increased by either decreasing alkalinity or increasing temperature [3][4]. While stray current can lead to serious corrosion of the reinforced steel embedded in concrete, no experiments have shown that there are notable effects of stray current on either the alkalinity of the pore solution or the temperature of the concrete. Given this, chloride ion stability when found in FS should be independent of stray current.

3.3 Release of chloride ions adsorbed by C-S-H gel

There was a significant effect of stray current on changes to C-S-H gel R_{cl} values, which decreased with both increasing DC loading time and voltage (Figs. 6 and 7). Moreover, C-S-H gel R_{cl} value profile was also similar to that seen for HCP. As such, it is likely that the release of chloride ions adsorbed by C-S-H gel was the main reason for the release of bound chloride ions in HCP after the application of stray current.

4. DISCUSSION

As stated in Section 3.3, the effect of stray current on the release of bound chloride ions is primarily related to the C-S-H gel. While there are several theories used to interpret the mechanism behind chloride ion adsorption in C-S-H gels, the EDL theory is thought to be the most accurate and widely applicable [23-27].

As early as 1879, Helmholtz proposed the gel EDL model. Stern then revised this model and established the Stern model of EDL, which divides EDL into two parts: the Stern and diffusion layers. The formation of the Stern layer can be attributed to specific adsorption patterns, which consist of electrostatic and vander Waals attractive forces. The latter enables ions to further adhere to the surface of a given solid. As a result of these attractive forces, ions can be stably adsorbed on the surface of a given solid to form the Stern layer. The thickness of the Stern layer is determined by the size of adsorbed ions, and it is usually about one to two molecules thick. The interface between the Stern and diffusion layers is named the Stern plane. In an electrical field, a new plane will be formed that is different from Stern plane and is named the shear plane.

According to the Stern model, the application of an electrical field results in a dramatic drop of the surface potential of the solid surface from φ_0 to φ_σ. It will finally drop to ζ, where φ_σ and ζ are the potentials for Stern and shear planes, respectively. In low concentrations of a given electrolyte solution, ζ can be approximated as φ_σ, which can be quantified using zeta potential instrumentation. Given this, changes to ζ are very useful measurements for the evaluation of changes to EDL.

Grahame further divided the Stern layer into two parts. Since the ions adsorbed through a specific adsorption do not occur during a hydrated reaction, they are closer to the surface of the solid. Given this, the location occupied by these ions is named the inner Helmoltz plane (IHP). The location where the diffusion layer starts is named the outer Helmoltz plane (OHP). Ions that have unlike charges with respect to the solid's surface can easily enter the Stern layer due to electrostatic and van der Waals attractive forces. This results in decreased absolute values for both φ_σ and ζ. It is difficult for ions with like charges with regards to the solid's surface to approach due to electrostatic repulsion. However, when van der Waals attractive forces are enough to overcome electrostatic repulsion, they can also enter the Stern layer. This would also result in increased absolute values for both φ_σ and ζ.

4.1 ζ variation in HCP after loaded DC

HCP consists of many phases, with portlandite possessing a positive surface charge while other phases (e.g. C-S-H, ettringite, and calcite) possess a negative surface charge [18]. The HCP zeta potentials resulting from distilled water and 0.5 MNaCl solution and after standard curing for 28 d are shown in Fig.9. Owing to the fact that a solution of NaCl was used as the mixing water, there was an obvious decrease of ζ from -40.071 mV to -50.804 mV. Fig.9 (a) shows the change in HCP ζ potentials made with NaCl solution and after loading with 20 V DC for 2, 4, and 6 days. As indicated, longer loading time resulted in increased ζ potentials. Notably, the relationship between the change in ζ and the loading time was nearly linear.

The effect of DC voltage on HCP ζ potentials made with NaCl solution is plotted in Fig. 9(b). As shown, ζ increased with increasing voltage. These results further demonstrated that stray current changed the stability of ions bound to the surface of the hydration products of HCP.
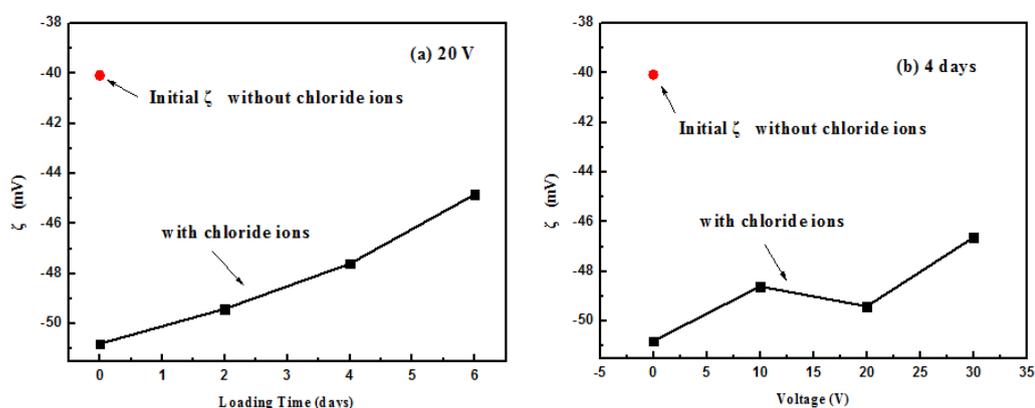
Figure 9. The effect of stray current on ζ of HCP: (a) loaded 20 V DC for 2, 4 and 6 days; (b) loaded 10, 20 and 30 V DC for 4 days

4.2 Mechanism behind chloride ion adsorption on C-S-H gel

Some researchers have proposed an ion exchange theory to explain the adsorption of chloride ions on C-S-H gels. According to this theory, calcium ions are neutralized of their negative charge

prior to entering the EDL of the C-S-H gel. After this, the hydroxyl ions from the C-S-H gel are replaced by chloride ions, which can be explained by the following equation [25][28]:

$$C - S - H - OH^-_{(s)} + Na^+ + Cl^- \leftrightarrow C - S - H - Cl^-_{(s)} + Na^+ + OH^- \qquad (5)$$
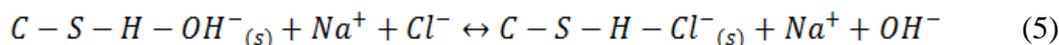
Where the subscript (s) stands for the solid phase. However, earlier reports by Suryavanshi and colleagues found that the quantity of OH⁻ released into the pore solution was not equal to the quantity of bound chloride ions seen during hydration. This was despite the fact that the anion-exchange reaction between the Cl⁻ in pore solution and OH⁻ in the inter-layers of the AFm hydrates to form FS was the main reason for the release of OH⁻ [29].

At alkaline conditions, the silanol site (e.g.SiOH) of the C-S-H gel surface will be dissociated, which becomes more notable with increasing calcium hydroxide concentration[30]. As a result and as indicated by Eq. 6, the C-S-H surface has negative charges [18][31]:

$$SiOH + OH^- \leftrightarrow SiO^- + H_2O \qquad (6)$$
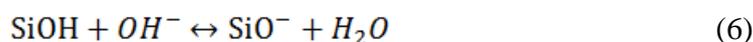
Viallis-Terrisse and colleagues hypothesized that when the C-S-H gel and NaCl solution interacted, Na⁺ and Cl⁻ were likely to behave as indifferent electrolytes toward the C-S-H surface. This meant that both Na⁺ and Cl⁻ would not be adsorbed onto the C-S-H gel surface[31]. However, Elakneswaran argued that only Na⁺ behaved as an indifferent ion towards to the C-S-H gel surface and Cl⁻ could be bound by unionized SiOH. This is explained by the following Eq.(7) [18].

$$SiOH + Cl^- \leftrightarrow SiOHCl^- \qquad (7)$$

According to Eq. 7 and owing to the ionization of SiOH, the surface of the C-S-H gel has negative charges. This means that Cl⁻ will be repelled by it. With increasing pH, SiOH ionization becomes more notable. This results increased negative charges on the surface of the C-S-H gel. The electrostatic repulsion between the C-S-H gel surface and Cl⁻ increases, magnifying the difficulty of Cl⁻ to approach the C-S-H gel surface. This may partly explain why chloride binding is reduced with increasing pH [32-34]. Nevertheless, parts of chlorides also can enter into the EDL of the C-S-H gel to be adsorbed ontoits surface (Eq. (7)). This can occur when the van der Waals attractive forces between unionized SiOH and Cl⁻ is large enough to overcome its corresponding electrostatic repulsion.

The relationship between ζ and the adsorbed chloride ions of the C-S-H gel after it was immersed in NaCl solution for 1, 7, and 14 d is shown in Fig.10. As indicated, there was an adsorptive action of chloride ions onto the C-S-H gel, Moreover, the quantity of adsorbed chloride ions increased with increasing immersion time. As shown in Fig.10, the value of ζ was also inversely proportional to the quantity of adsorbed chloride ions. This finding is in agreement with previous results reported by Elakneswaran and colleagues [18].

According to both the Stern and Grahame models, ζ is evident as the potential of the Stern layer. This means that ζ equals φ_δ. Therefore, it can be concluded that the adsorbed chloride ions are not only in the diffusion layer, but also in the Stern layer. Inclusion in the Stern layer results in the decreased C-S-H gel ζ value (Fig.10).It should also be noted that because of the limited space and the stronger electrostatic repulsion found in the Stern layer, the adsorbed chloride ions should be primarily distributed at the diffusion layer of the C-S-H gel.
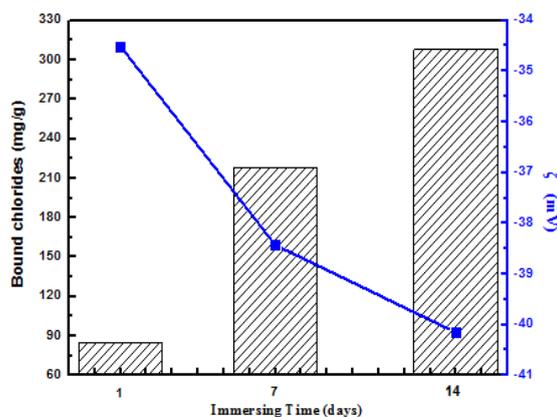
Figure 10. The relationship between ζ and bound chlorides after C-S-H gel was immersed in NaCl solution for 1, 7 and 14 days

4.3 Effect of stray current on the stability of adsorbed chloride ions in the EDL

As stray current flows through rebar in concrete structures, an electrical field will be formed around the reinforcing steel and ions in the pore solution of the concrete will migrate. Previous work has investigated the migratory characteristics of chloride ions in concrete after the application of stray current [35]. These results showed that chloride ions had accelerating migration to the surface of the reinforced steel in the concrete (Fig.11), indicating that there is a strong attractive force between the electrical field and chloride ions. Since the adsorbed chloride ions in the diffusion layer were mainly related to thermal motion, they were first released from the EDL of the C-S-H gel. In the case of the adsorbed chloride ions in the Stern layer, results indicated that they were more stable when compared with those in the diffusion layer. This might be because they were adsorbed on the unionized SiOH through specific adsorption. Fig.12 shows the changes in ζ of the C-S-H gel surface after the application of stray current. As expected, ζ of the C-S-H gel surface increased not only with longer application of the electric field, but also with increasing voltage. This coincided with changes in HCP ζ after application of stray current (Fig.10). It is probably that the increase of ζ is related to the release of adsorbed chloride ions in the Stern layer. This also demonstrates that the van der Waals attractive forces between the unionized SiOH and Cl⁻ was too weak to overcome the electric field force that kept Cl⁻ on the surface of the C-S-H gel. Given this, it can be concluded that chloride ions are in both the Stern and diffusion layers and that they can be released from C-S-H with the application of stray current.

It should be noted that the application of an electrical field will decrease the thickness of the EDL [36], resulting in decreased ions in the EDL. This is especially true for the Stern layer. As a result, it is difficult for chloride ions to re-enter the EDL after DC application has stopped. This is the likely reason behind the long-term effect of stray current on the stability of bound chloride ions(Fig.8).
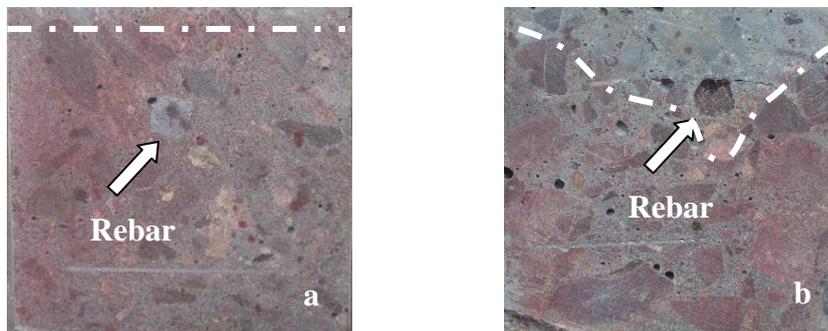
Figure 11. Zone of chloride ion permeated: (a) without stray current; (b) with stray current[36]
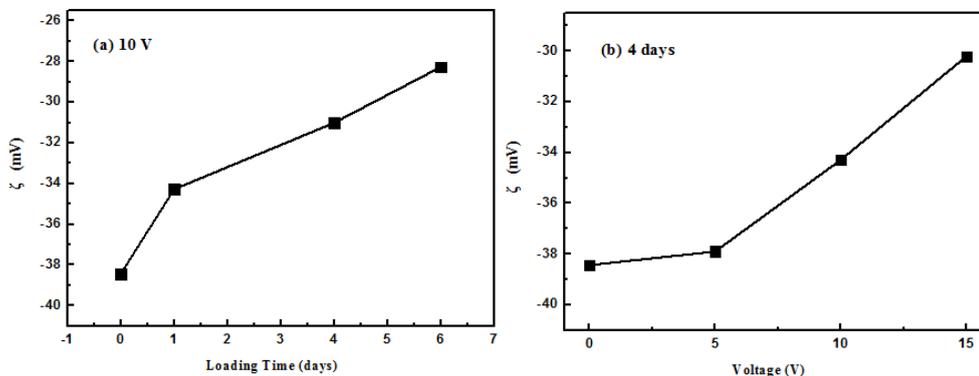
Figure 12. The change in ζ of C-S-H surface after loaded stray current: (a) loaded 10V DC for 1, 4 and 6 days; (b) loaded 5, 10 and 15 V DC for 4 days

5. CONCLUSION

Stray current is a common phenomenon of current leakage and is often seenin the reinforced structures used in urban railway networks. Not only does it induce serious corrosion of the reinforced steel in such concrete structures, but it also affects the migration and binding of chloride ions. As such, this investigation sought to evaluate the effect of stray current on the release of bound chloride ions in cement paste. The mechanism behind the release of bound chloride ions was then analyzed and discussed based on the EDL theory and ζ results. The main conclusions drawn were as follows:

(1)   There was a negative and long-term effect of stray current on the stability of bound chloride ions in cement pastes. This effect became more serious with both increased loading time and DC voltage. However, we showed that the effect of low DC voltage (5 V) was negligible.

(2)   The stability of bound chloride ions when combined in FS should be independent of stray current. The release of bound chloride ions should also be attributed to the release of chloride

ions adsorbed by the C-S-H gel.

(3)	The adsorption of chloride ions induced changes in ζ of the C-S-H gel surface, indicating that adsorbed chloride ions were not only in the diffusion layer, but also in the Stern layer. This was due to the attractive force of the stray current's electrical field on chloride ions. The quantity of adsorbed chloride ions was inversely proportional to ζ on the C-S-H gel surface.

References

1.	L. X. Nie, J. Y. Xu and E. Bai, *Constr. Build. Mater.,* 165 (2018) 232.
2.	J. Xu, C. Zhang, L. Jiang, L. Tang, G. Gao and Y. Xu, *Constr. Build. Mater.,* 45 (2013) 53.
3.	J. Geng, D. Easterbrook, L.Y. Li and L.W. Mo, *Cem. Concr. Res.,* 68 (2015) 211.
4.	S. Goñi and A. Guerrero, *Cem. Concr. Res.,* 33 (2003) 21.
5.	J. Geng, L. W. Mo, *J. Chin. Ceram. Soc.,* 42 (2014) 500.
6.	K. Darowicki and K. Zakowski, *Corros. Sci.,* 46 (2004) 1061.
7.	W. Feng, J. X. Xu, P. Chen, L. H. Jiang, Y. B. Song and Y. L. Cao, *Constr. Build. Mater.,* 158 (2018) 847.
8.	G.X. Li, A. Zhang, Z.P. Song, S.J. Liu and J.B. Zhang, *Constr, Build. Mater.,* 158 (2018) 640.
9.	L. Bertolini, M. Carsana and P. Pedeferri, *Corros. Sci.,* 49 (2007) 1056.
10.	A. O. S. Solgaard, M. Carsana, M. R. Geiker, A. Küter and L. Bertolini, *Corros. Sci.,* 74 (2013) 1.
11.	Z. G. Chen, C. K. Qin, J. X. Tang and Y. Zhou, *J. Nat. Gas Sci. Eng..,*15 (2013) 76.
12.	X. H. Wang, X. H. Tang, L. W. Wang, C. Wang and W. Q. Zhou, *J. Nat. Gas Sci. Eng.,* 21 (2014) 474.
13.	A. Matthew, Y. Pu, V. Kirk, S. Gaurav and N. Narayanan, *Cem. Concr. Res.,* 66 (2014) 1.
14.	A. Pérez, M. A. Climent and P. Garcés, *Corros. Sci.,* 52 (2010) 1576.
15.	C. C. Yang, S. W. Cho, J. M. Chi and R. Huang, *Mater. Chem. Phys.,* 77 (2003) 461.
16.	M. Castellote, C. Andrade and C. Alonso, *Cem. Concr. Res.,* 29 (1999) 1799.
17.	H. Friedmann, O. Amiri, A and Aït-Mokhtar, *Cem. Concr. Res.,* 38 (2008) 1394.
18.	Y. Elakneswaran, T. Nawa and K. Kurumisawa, *Cem. Concr. Res.,* 39 (2009) 340.
19.	M. V. A. Florea and H. J. H. Brouwers, *Cem. Concr. Res.,* 42 (2012) 282.
20.	P. T. Nguyen and O. Amiri, *Constr. Build. Mater.*, 50 (2014) 492.
21.	A. K. Suryavanshi, J. D. Scantlebury and S. B. Lyon, *Cem. Concr. Res..*, 26 (1996) 717.
22.	K. D. Weerdt, D. Orsakova and M. R. Geiker, *Cem. Concr. Res.*, 65 (2014) 30.
23.	Y. Elakneswaran and T. Nawa, K. Kurumisawa, *Cem. Concr. Compos.*, 31 (2009) 72.
24.	H. Hirao, K. Yamada, H. Takahashi and H. Zibara, *J. Adv. Concr. Technol.*, 3 (2005) 77.
25.	J. J. Beaudoin, V. S. Ramachandran, R. F. Feldman, *Cem. Concr. Res.*, 20 (1990) 875.
26.	V. Baroghel-Bouny, X. Wang, M. Thiery, M. Saillio and F. Barberon, *Cem. Concr. Res.*, 42 (2012) 1207.
27.	P. T. Nguyen and O. Amiri, *Constr. Build. Mater.*, 50 (2014) 492.
28.	T. Zhang and O. E. Gjørv, *Cem. Concr. Res.*, 26 (1996) 907.
29.	A. K. Suryavanshi, J. D. Scantlebury and S. B. Lyon, *Cem. Concr. Res.*, 26 (1996) 717.
30.	C. Plassard, E. Lesniewska, I. Pochard and A. Nonat, *Langmuir.*, 21 (2005) 7263.

31. H. Viallis-Terrisse, A. Nonat and J. C. Petit, *J. Colloid Interface Sci.,* 244 (2001) 58.
32. Q. Yuan, C. J. Shi, G. D. Schutter, K. Audenaert and D. H. Deng, *Constr. Build. Mater.,* 23 (2009) 1.
33. Q. Zhu, L. H. Jiang, Y. Chen, J. X. Xu and L. L. Mo, *Constr. Build. Mater.,* 37 (2012) 512.
34. K. D. Weerdt, D. Orsakova and M. R. Geiker, *Cem. Concr. Res.,* 65 (2014) 30.
35. J. Geng, Q. J. Ding, J. Y. Sun and B.N. Sun, *J. Build. Mater.,* 13 (2010) 121.
36. H. Zhou, Y. M. Wang, H. C. Jiang and X. S. Chen, *J. Rare Earths,* 25 (2007) 80.